International Journal of Material Science Innovations (IJMSI) 2(3): 52-58, 2014
ISSN 2289-4063

Research Article

Effects Pre-strain of Carbon Steel on Stress-Strain Diagram in CO_2 Environment with the Presence of H_2S

Y. P. Asmara*, Juliawati, J. Jaafar, K. Azuar, J.P. Siregar, T. Kurniawan.

Faculty of Mechanical Engineering, Universiti Malaysia Pahang
Pekan 26600 Pahang Malaysia
Tel.; 6094246355; fax:6094246222
*E-mail address: YPanca@ump.edu.my

A b s t r a c t

Keywords:

CO_2 corrosion,
Response surface model,
Empirical model.

In oil and gas industrial environments, carbon dioxide (CO_2) and hydrogen sulfide (H_2S) contained in aqueous system are the most common corrosive factors which deteriorate infrastructure made of carbon steel. One of the key factors to accelerate corrosion rate is strain conditions of the steel. Higher strain is suspected to contribute on more hydrogen penetration. This research tested simultaneously the effects pre-strain of carbon steel under saturated CO_2 and CO_2/H_2S environment. The steels were tested in between 5 to 35 percents of initial pre-strain. It showed that the existence of H_2S decrease the ultimate tensile strength of the steel. While, the initial pre-strains condition increases the maximum tensile stress. In addition, CO_2 and H_2S contribute on decreasing toughness.

Accepted:18 June2014

1. Introduction

Hydrogen damage is one of the major causes of steel equipment failures in the oil and gas industry especially pipelines and pressure vessels [1]. It is caused by the dissolution of atomic hydrogen in the steel, as a result of the cathodic reduction of proton (H^+) which accompanies the anodic oxidation of iron in acid media. The key factors determine for the corrosion rate are: sensitization of material, stress-stress applied, and corrosion environment.

Several failure modes can occur in service, for example (a) Hydrogen induced cracking (HIC) which is corresponds to internal cracks generated by the recombination of hydrogen to gaseous molecules at certain appropriate traps in the steel, like manganese sulfide (MnS) inclusions or pearlite bands [2]. This failure mode usually occurs in the absence of externally applied stresses [2,4,5] and develops mainly parallel to the steel surface [4-6], appearing mostly in the pattern of stepwise subsurface cracks as shown in figure 2 [4]. (b) Sulphide stress cracking (SSC) occurs when hydrogen sulfide (H_2S) and water are present [2]. This cracking mode is generated from the surface of the steel and requires an applied stress [2,4, 7-9]. H_2S is known to have an aggravating influence to the cracking. The selection of steels for oil and gas environments containing H_2S thus requires appropriate testing, to ensure resistance to cracking in the field conditions [2].

Effects of plastic deformation on the corrosion behavior play an important role to the corrosion current densities and polarisation resistance that can change microstructure dislocation. Dislocations occur when level of pre-stains are changed. In CO_2/H_2S systems, film properties can control the rate of degradations and cracks growth. The tarnish film that formed at the crack tip is periodically ruptured, and the bare metal at the crack tip corrodes periodically in the solution to induce the growth of the crack [17–20]. The galvanic current tests stated that growth and rupture cycles of the film at crack tip during corrosion growth involves stress at the ahead of crack and dislocation movement from the crack tip generated on the specimen surface to crack the tarnish film.

2. Research methodologies

2.1. Specimens

The specimens were carbon steel with chemical composition is as shown in Table 1. The geometry of the specimens was as follows: gauge length: 25 mm, and diameter: 6 mm. All of the specimens were abraded with silicon carbide paper (1000 grit), degreased with acetone, and subsequently washed in distilled water. Samples were applied pre-strained under tension to strains of 5%, 17%, 30% and 35%.

Table 1: Composition of 080A15 (BS 970) carbon steel used in the experiments

Steel	C (%)	Si (%)	Mn (%)	P (%)	S (%)	Cr (%)	Ni (%)
080A15	0.14	0.175	0.799	0.01	0.03	0.06	0.065

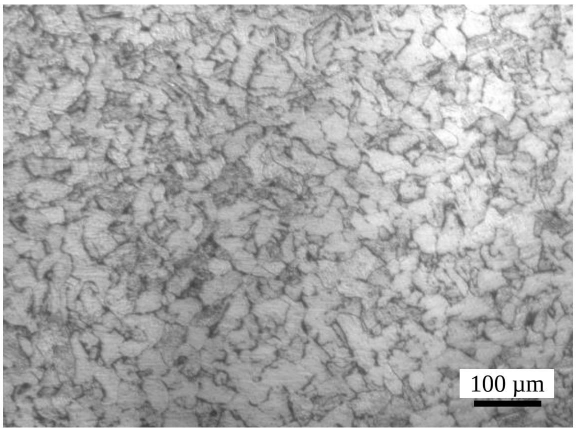

Fig.1: Micro structure of sample used in experiments.

.

2.2. Electrochemical set-up to corrosion test

A typical schematic three-electrode set-up used in all electrochemical test. Glass cell was fitted with graphite electrodes as auxiliary electrode and a Ag/AgCl as a reference electrode. All experiments were conducted in 1-litre glass cell equipped with Ag/AgCl reference electrode and stainless steel as the auxiliary electrode. CO_2 gas was purged for 1 hour into 3% sodium chloride solution at 1 bar pressure for 1 hour.

2.3. Cell solutions

The experiments were performed in stagnant condition. The total pressure was 1 bar, the glass cell was filled with 1 liter of distilled water and 3% wt NaCl which was stirred with magnetic stirrer. Then, CO_2 gas was bubbled through the cell (at least one hour prior to experiments) in order to saturate and de-aerate the solution. 1 mol H_2S gas was added by mixing Na_2S and H_2SO_4 into 3% of NaCl solution. The linear polarization resistance (LPR) technique was used to measure the corrosion rate. The procedure is similar to ASTM Experimental test G 5-94 [9].

3. Results and discussions

3.1 Stress-Strain Diagram

Table 2: Effects of pre-strain on tensile test properties

Compositions	5%			17%			30%			35%		
	ε (mm)	Y_s (MPa)	U_s (MPa)	ε (mm)	Y_s (MPa)	U_s (MPa)	ε (mm)	Y_s (MPa)	U_s (MPa)	ε (mm)	Y_s (MPa)	U_s (MPa)
Blank	20	10.5	13	18	13	13	16	13	12	14	13	13
CO_2	18	11.5	13.2	17	13	13	15	13	13	12	14	13
CO_2/H_2S	15	13.5	13.4	10	14	14	9	13.5	14.5	7	14.5	13.5

Table 2 shows effects of pre-strain on mechanical properties of the samples which were taken from tensile test. It states, generally, indications of decreasing elongation of the tensile test before fracture due to CO_2 and H_2S. Effects of increasing pre-strain show that the higher pre-strain causes the maximum elongation of samples will decrease. Stress-strain curve of the pre-strained specimens at room temperature are given in Figure 2. In this experiment, the specimens elongation were fix at 0, 5%, 17%, 30%, 35%. The applied stress corresponding to the elongation is presented at Table 2.

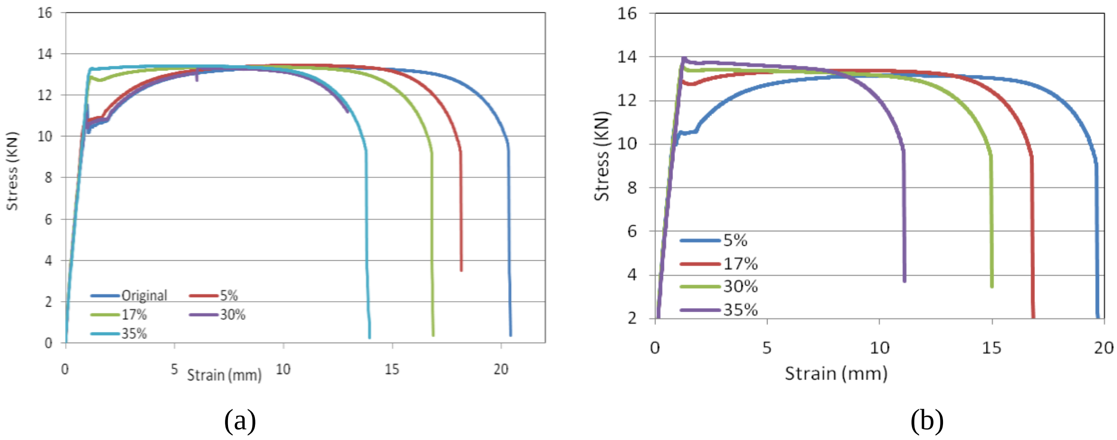

Fig.2: Effects of pre-strain on stress-strain graph in blank solution (a) and solution containing saturated CO_2/ H_2S gas (b).

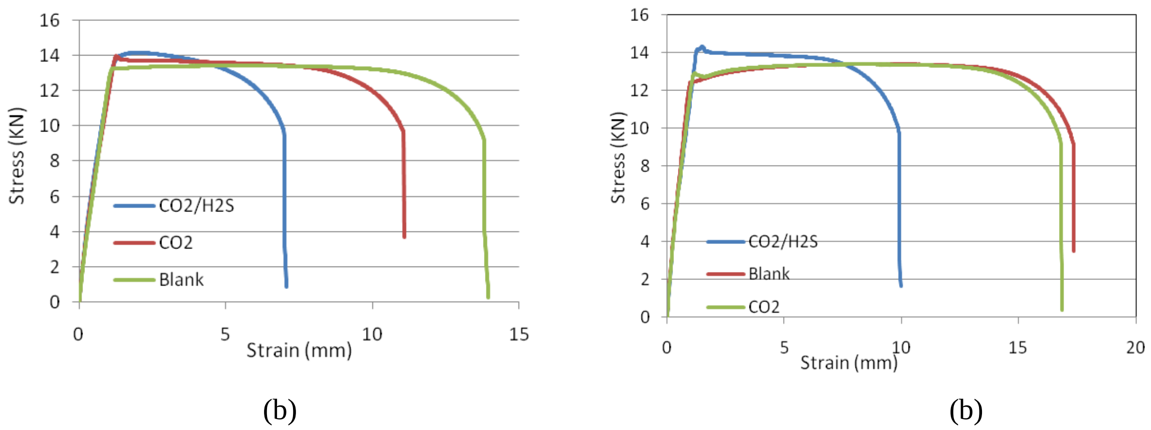

Fig.3: Effects of CO_2 and CO_2/ H_2S gas on stress-strain graph at conditions of 17 % (a) and 35 % (b) pre-strain.

Figure 3 shows the relation between the strain of 17% and 35% corresponding to 2.3 kN and 4.9 kN the applied stress at 25 °C. From the results shown in Figure 3, it is shown that the pre-strains caused higher in maximum tensile strength and reduce elongation. From the Figure 3, it was described that effects of pre-strain, CO_2 and H_2S decreased elongations that can be related decreasing toughness strength (Figure 4). It was indicated that the materials have reached plastics deformations during the starin.

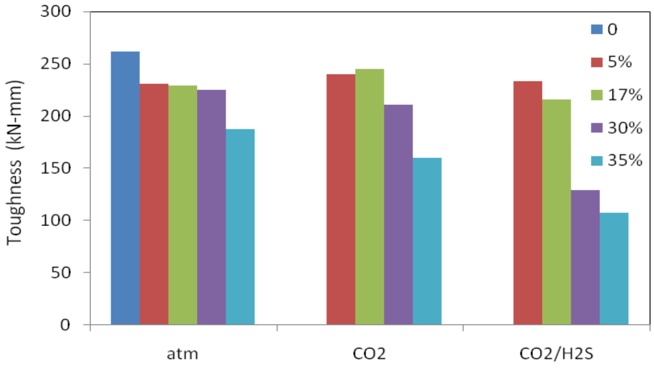

Fig.4: Effect of pre strain on samples toughness at atmosphere, CO_2 and CO_2/H_2S environmental conditions.

3.2 Corrosion rate

Total corrosion rate (mass loss) of samples after immersed for three days at solutions containing CO_2 and CO_2/H_2S is presented at Figure 5. Total mass/weight loss can be determined from the difference weight of samples before and after immersing time. Figure 5 shows that total mass loss will increase with increasing pre-strain. At the lower of pre-strain (less than 10%) effects of CO_2 was dominant in increasing mass loss. At higher pre-strain (more than 10%), effects of H_2S contributed to higher mass loss.

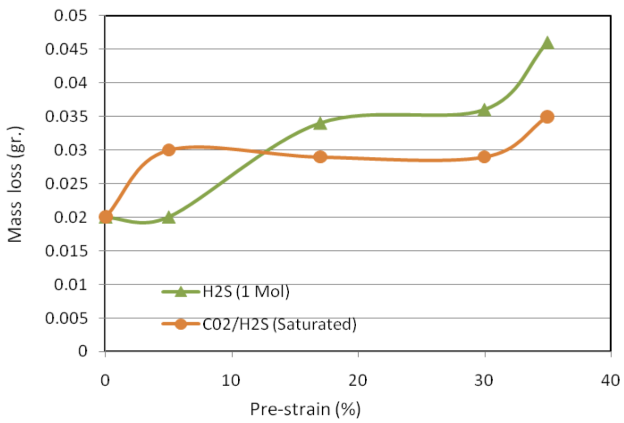

Fig.5: Effects of pre-strain at conditions with H_2S and CO_2 on mass loss

4 Conclusions

Based on experimental studies, it can be concluded several finding as follows:

- Pre-strains increase maximum tensile stress and decrease elongation and also decrease toughness.
- CO_2 and H_2S contribute on decreasing toughness.
- In solution containing CO_2 and H_2S with strain of 5%, 17% and 35%, materials have reached plastics deformation.
- At low pre-strain, the effects of CO_2 in increasing corrosion rate are more dominant as compared to the effects of H_2S. The dominant effect of H_2S was observed at high pre-strain.

Acknowledgments

This work was conducted under internal research grant Universiti Malaysia Pahang RDU 120337.

References

[1] Nesic S. Key Issues Related to Modelling of Internal Corrosion of Oil and Gas Pipelines – *A* review. *Corrosion Science* 2007; 49: 4308 – 4338,

[2] Nordsveen, S.N., R. Nybor., A. Stangeland A Mechanistic Model for Carbon Dioxide Corrosion of Mild Steel in The Presence of Protective Iron Carbonate Films—Part 1: Theory and Verification. *Corrosion* 2001; 59: 5 - 6.

[3] Schmitt MM, Papenfuss M. Understanding Localized CO_2 Corrosion of Carbon Steel From Physical Properties of Iron Carbonate Scales Fracture Mechanical Properties of Iron Carbonate Scales. *NACE International Corrosion proceeding* 1999; 38.

[4] Nafday O. Film Formation and CO_2 Corrosion in The Presence of Acetic Acid. Master thesis of Ohio University, 2004.

[5] Zhang G. On The Fundamentals of Electrochemical Corrosion of X65 steel in CO_2-Containing Formation Water in The Presence of Acetic Acid in Petroleum Production. *Corrosion Science* 2009; 51: 87–94.

[6] Amri J, Gulbrandsen E, Nogueira. The Effect of Acetic Acid on The Pit Propagation in CO_2 Corrosion of Carbon Steel. *Electrochemistry Communications* 2008; 10: 200–203.

[7] Martin C.F. Prediction CO_2 Corrosion with the Presence of Low concentration Acetic Acid in Turbulent Flow Conditions. *Master Thesis of UTP* 2009.

[8] Mokhtar I. C. Prediction CO_2 corrosion with The Presence of Acetic Acid, *PhD theses* of *UMIST* 2005.

[9] ASTM G 5-94 - Standard Reference Test Method for Making Potentiostatic and Potentiodynamic Polarization Measurements.

[10] Wei Sun. Kinetics of Iron Carbonate and Iron Sulfide Scale Formation in CO_2/H_2S Corrosion, *PhD Thesis of Ohio University* 2006.

[11] Minitab Inc. Minitab Statistical Software Release 15 for Windows. State College, Pennsylvania 2006.

[12] Andrzej Anderko, Robert D, Young. Simulation of CO_2 / H_2S Corrosion Using Thermodynamic and Electrochemical Models. *NACE International Corrosion preceding* 1999: 31.

[13] George KS, Nesic S. Electrochemical Investigation and Modeling of Carbon Dioxide Corrosion of Carbon Steel in The Presence of Acetic Acid. *NACE International Corrosion proceeding* 2004: 4379.

[14] George KS., Nesic S. Investigation of Carbon Dioxide Corrosion of Mild Steel in The Presence of Acetic Acid— Part 1: Basic Mechanisms, Corrosion, *NACE International Corrosion proceeding* 2007: 4379.

[15] Box GEP, Draper NR. Empirical Model Building and Response Surfaces. *John Wiley and Sons*, New York, 1987.

[16] Devore, Peck. Statistics, The Exploration and Analysis Data, fifth edition, Thomson Learning, Belmont 2005.

[17] Hedges B LM. The Role of Acetate in CO_2 Corrosion: The Double Whammy. *NACE International Corrosion proceeding* 1999.

[17] Free Corp. Corrosion prediction model, WWW.Ohio Model. Institute Corrosion and Multi phase.

[18] ECE corrosion program software www.intetech.com

[19] Tracey S., Jackson, E. Patrick, Martin, Rhonda, P., Surface Response Design to Study the Effect of Low Oxygen Levels on Carbon Dioxide Corrosion Environments, *NACE International Corrosion Proceeding* 2009: 9574.

[20] Gulbrandsen E. Acetic Acid and Carbon Dioxide Corrosion of Carbon Steel Covered with Iron Carbonate. *NACE International Corrosion proceeding* 2007: 7322.